08

Solid-phase synthesis of plasmonic hybrid nanoparticles Ag−Ag_2Se

© V.Ya. Kogai, G.M. Mikheev

Udmurt Federal Research Center, Ural Branch Russian Academy of Sciences, Izhevsk, Russia
E-mail: vkogai@udman.ru

Received August 15, 2025
Revised August 15, 2025
Accepted August 29, 2025

It has been shown for the first time that during the formation of the Ag/Se thin-film structure, as a result of Ag diffusion into the Se film and the course of a solid-phase chemical reaction, a hybrid plasmonic material containing a core of metallic silver nanoparticles with a shell of semiconductor Ag_2Se nanoparticles in an amorphous selenium matrix is formed. It is shown that the extinction spectrum obtained by spectroscopic ellipsometry shows the presence of two maxima in the blue and red regions of the optical spectrum, corresponding to localized surface plasmon resonances. It was found that the non-annealed synthesized films have high values of the extinction coefficient $k = 5.0$ at $\lambda = 883$ nm and the refractive index $n = 7.2$ at $\lambda = 1074$ nm.

Keywords: thin-film structures, solid-phase chemical reaction, hybrid nanoparticles, plasmon resonance.

DOI: 10.61011/TPL.2026.01.62812.20473

Rapid development of modern nanotechnology opens up wide opportunities for combining various nanocrystals with different characteristics into a single superstructure. Metal/dielectric and metal/semiconductor composite nanostructures are of considerable interest in this context [1,2]. Hybrid nanostructures with a dielectric core (e.g., SiO_2) coated with a thin noble metal layer feature unique optical properties that were examined in [3,4].

Research into the optical properties of hybrid nanostructures consisting of metal core nanoparticles and a shell of nanoclusters of organic molecules characterized by a high degree of ordering has also advanced rapidly [5–8].

Hybrid nanostructures composed of a noble metal and a heavily doped *n*- or *p*-type semiconductor with both components having plasmonic properties have attracted increasing attention in recent years. This leads to a significant change in physicochemical characteristics of hybrid nanocomposites (specifically, to an improvement of their photocatalytic properties [9,10]). When both localized surface plasmon resonances are excited, a significant local electric field enhancement is observed at the interface in such hybrid nanocomposites (compared to the case of excitation of a noble metal or a semiconductor material only).

Plasmonic metal-semiconductor materials based on noble metals and copper chalcogenides were reviewed in [11], where the approaches to synthesis of such materials with controlled plasmonic properties were summarized.

The most simple and technologically advanced method for synthesis of hybrid nanostructures containing a noble metal and a semiconductor was proposed in our study [12]. Its potential was illustrated through the example of synthesis of Cu−$CuAsSe_2$ hybrid nanoparticles with sequential deposition of Cu and As_2Se_3 on a glass substrate in a single vacuum cycle. Following diffusion of Cu into an As_2Se_3 film and a solid-phase chemical reaction between Cu and As_2Se_3, a hybrid nanostructure with Cu nanoparticles encapsulated in a glassy $CuAsSe_2$ shell was formed. In a similar fashion, hybrid Ag−Ag_2Se nanoparticles may be obtained when a thin-film Ag/Se structure is formed in a vacuum chamber via diffusion of Ag into a Se film and a solid-phase chemical reaction between Ag and Se. They may consist of nanoparticles of a metal Ag core and semiconductor nanoparticles of an Ag_2Se shell, which provide an opportunity to observe plasmon resonances and are relevant in the context of synthesis of a new material with unique optical properties.

The aim of the present study is to examine the influence of Ag film thickness in an Ag/Se thin-film structure and thermal annealing on the plasmon resonance and optical properties of synthesized films.

Thin-film Ag/Se structures were formed in a working chamber under vacuum (10^{-3} Pa) at a glass substrate temperature of 298 K. The thickness of the Se film was the same in all samples (50 nm), while the Ag film thickness was 12, 25, or 35 nm.

X-ray diffraction analysis of the synthesized films was carried out using a D2 PHASER (Bruker) diffractometer with CuK_α radiation (at a wavelength of 0.1541 nm).

The optical properties of films were studied using a SENresearch 4.0 SER 850 (SENTECH Instruments GmbH) spectroscopic ellipsometer within a wide range of wavelengths from 240 to 2500 nm.

The synthesized films were annealed in a SNOL-3.5 furnace in air at a temperature of 140 °C for an hour.

Figure 1 shows the diffraction patterns of unannealed Ag (12 nm)/Se (50 nm), Ag (25 nm)/Se (50 nm), and Ag (35 nm)/Se (50 nm) film structures. One low-intensity diffraction peak from the orthorhombic Ag_2Se phase at angle $2\theta = 40.4°$ (PDF 89-2591) is seen in the diffraction pattern of the Ag (12 nm)/Se (50 nm) sample (curve *1* in Fig. 1). Diffusing into the amorphous Se film, fine-dispersed Ag nanoparticles undergo a solid-phase chem-

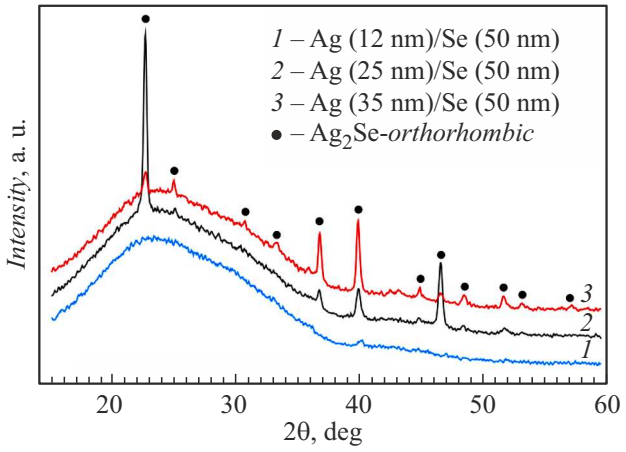

Figure 1. Diffraction patterns of the as-prepared film structures containing Ag films of different thicknesses.

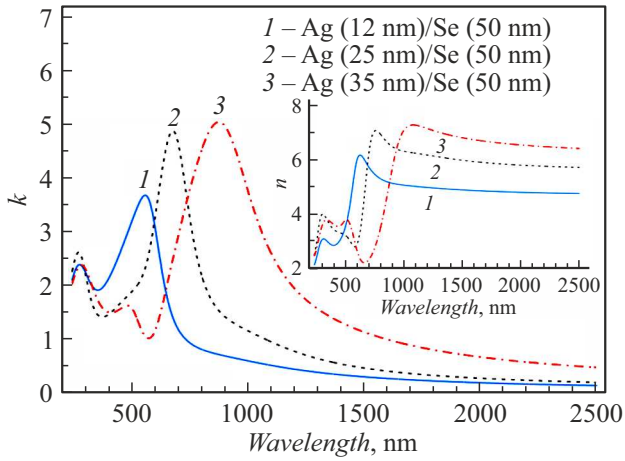

Figure 3. Dependences of extinction coefficient k and refraction index n (inset) on wavelength λ of incident light for as-prepared film structures containing Ag films of different thicknesses.

ical reaction with Se and form the Ag_2Se compound. The concentration of Ag_2Se nanoparticles increases with increasing Ag film thickness, which leads to the emergence of a large number of high-intensity diffraction peaks from the orthorhombic Ag_2Se phase (PDF 89-2591) in the diffraction patterns of the Ag (25 nm)/Se (50 nm) and Ag (35 nm)/Se (50 nm) samples (curves *2*, *3* in Fig. 1).

Selenium remains amorphous in all the as-prepared unannealed samples; therefore, peaks from the crystalline phase of selenium are not observed in the diffraction patterns. Diffraction peaks from the crystalline Ag phase are also lacking, since Ag nanoparticles diffusing into the Se film are small in size.

When the as-prepared Ag (12 nm)/Se (50 nm), Ag (25 nm)/Se (50 nm), and Ag (35 nm)/Se (50 nm) samples are annealed, the orthorhombic Ag_2Se phase in the synthesized film is joined by hexagonal Se, which is evidenced by the emergence of diffraction peaks at

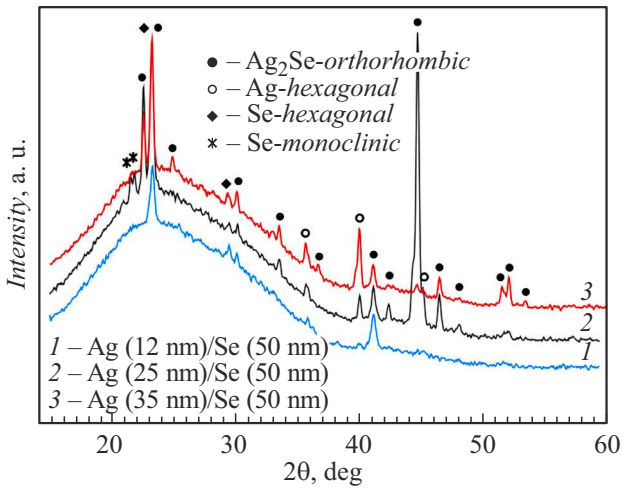

Figure 2. Diffraction patterns of the annealed film structures containing Ag films of different thicknesses.

angles $2\theta = 23.5$ and 29.7° (PDF 06-0362); hexagonal Ag (peaks at angles $2\theta = 35.9$, 40.3, and 45.3°, PDF 41-1402); and monoclinic Se (peaks at $2\theta = 21.6$ and 21.8°, PDF 76-1865) (curves *1–3* in Fig. 2).

Fine-dispersed silver coagulates during annealing, transforming into larger Ag nanoparticles. This is evidenced by the emergence of diffraction peaks from crystalline hexagonal Ag phases in the Ag (12 nm)/Se (50 nm), Ag (25 nm)/Se (50 nm), and Ag (35 nm)/Se (50 nm) samples (curves *1–3* in Fig. 2).

Apparently, a small fraction of silver does not undergo a solid-phase chemical reaction to form the Ag_2Se compound and remains in the nanoparticle form. The average crystallite sizes calculated using DIFFRAC.EVA in the Ag (35 nm)/Se (50 nm) sample were 22 nm for Se, 30 nm for Ag, and 34 nm for Ag_2Se.

Figure 3 shows the spectra of extinction coefficients $k(\lambda)$ and refraction index $n(\lambda)$ of the studied Ag (12 nm)/Se (50 nm), Ag (25 nm)/Se (50 nm), and Ag (35 nm)/Se (50 nm) film structures recorded before their thermal annealing. It is evident from Fig. 3 that spectral dependences $k(\lambda)$ for the as-prepared samples have two maxima, which are characteristic of the effect of localized surface plasmon resonance, within the 320–890 nm wavelength range. The maxima of plasmon peaks for hybrid Ag–Ag_2Se nanoparticles are at 442 and 883 nm (curve *3* in Fig. 3). The left peak is positioned quite close to the peak induced by the localized surface plasmon resonance of an uncoated silver particle. The right peak is significantly more intense than the left one. This is attributable to the difference between the excitation energy of an exciton in the Ag_2Se shell and the plasmon resonance energy in the Ag core. Double plasmon resonance was observed in spherical nanostructures consisting of a metal core and two shells (dielectric and metal). Numerical modeling of the optical properties of such structures revealed that when the plasmon resonances of the core

and the metal shell match spectrally, the electromagnetic wave field is amplified locally by a factor up to 10^4, and the scattering cross section increases by a factor up to 10^3 [13].

Fine-dispersed Ag nanoparticles may emerge during diffusion of Ag into a Se film in the process of relaxation of the elastic stress energy in the film. The kinetics of reaction diffusion of Ag into a Se film during relaxation of the elastic stress energy was investigated in our study [14]. The feasibility of a solid-phase chemical reaction activated by the elastic stress energy was demonstrated using the example of a Cu/As_2Se_3 film structure [15]. As a result of diffusion, fine-dispersed Ag nanoparticles are completely immersed in the amorphous selenium matrix and, coming into contact with selenium, undergo a solid-phase chemical reaction with the formation of the Ag_2Se compound on the surface of Ag nanoparticles. Hybrid Ag–Ag_2Se nanoparticles may be synthesized this way.

With an increase in thickness of the Ag film in the Ag/Se thin-film structure, the plasmon peak intensity for the Ag (35 nm)/Se (50 nm) sample increases to $k = 5.0$ at $\lambda = 883$ nm and shifts to the red spectral region (curve *3* in Fig. 3). This is attributable to an increase in concentration of hybrid Ag–Ag_2Se nanoparticles in the amorphous selenium matrix.

The refraction index in the as-prepared Ag (12 nm)/Se (50 nm), Ag (25 nm)/Se (50 nm), and Ag (35 nm)/Se (50 nm) film structures also increases with increasing thickness of the Ag film and reaches its maximum value of $n = 7.23$ at wavelength $\lambda = 1074$ nm for the Ag (35 nm)/Se (50 nm) sample (curve *3* in the inset to Fig. 3). The coexistence of fine-dispersed Ag nanoparticles and larger Ag_2Se nanoparticles in the synthesized film translates into polydispersity of the film system. Polydispersity grows more profound with increasing thickness of the Ag film in the Ag/Se thin-film structure, which, in turn, leads to an increase in refraction index. High refraction index values (from 5.5 to 7) within the 3000–6000 nm wavelength range were found in three-dimensional isotropic gold metamaterials [16].

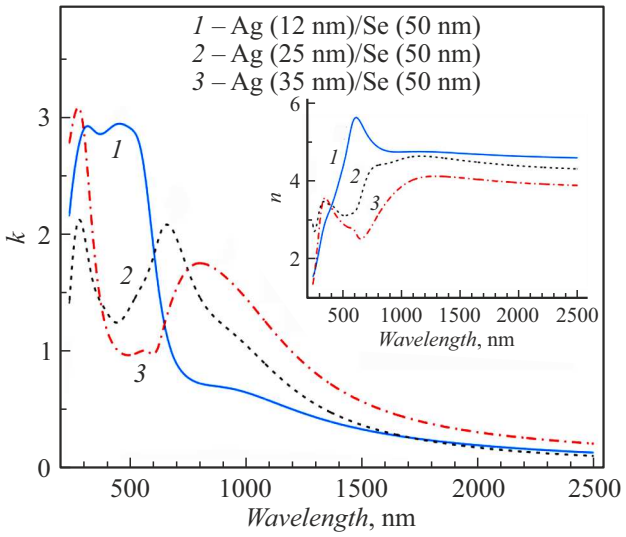

Figure 4. Dependences of extinction coefficient k and refraction index n (inset) on wavelength λ of incident light for annealed film structures containing Ag films of different thicknesses.

Figure 4 shows the spectra of extinction coefficients $k(\lambda)$ and refraction index $n(\lambda)$ of the studied Ag (12 nm)/Se (50 nm), Ag (25 nm)/Se (50 nm), and Ag (35 nm)/Se (50 nm) film structures recorded after their thermal annealing. It is evident from Fig. 4 that the plasmon peak in the samples with the maximum Ag film thickness (35 nm) decreases in intensity to $k = 1.8$ at $\lambda = 803$ nm and becomes broader (curve *3* in Fig. 4). This is induced by acceleration of the solid-phase chemical reaction between Ag and Se with the formation of the Ag_2Se phase (and the corresponding increase in its concentration) and amalgamation (coalescence) of fine-dispersed Ag nanoparticles into larger Ag nanoparticles, which is evidenced by the diffraction peaks from hexagonal Ag phases (curves *1–3* in Fig. 2). The refraction index in the annealed Ag (12 nm)/Se (50 nm), Ag (25 nm)/Se (50 nm), and Ag (35 nm)/Se (50 nm) film structures decreases with increasing thickness of the Ag film in the Ag/Se thin-film structure, dropping to $n = 4.07$ at $\lambda = 1148$ nm for the Ag (35 nm)/Se (50 nm) sample (curve *3* in the inset to Fig. 4). Polydispersity of the film system becomes less profound after annealing, and the refraction index values decrease.

Thus, hybrid Ag–Ag_2Se nanoparticles containing a metallic Ag core and a semiconductor Ag_2Se shell in an amorphous selenium matrix have been synthesized for the first time in the process of formation of a thin-film Ag/Se structure in a single vacuum cycle. Localized surface plasmon resonances were observed in the obtained hybrid Ag–Ag_2Se nanoparticles. The frequency positions and intensities of plasmon peaks in Ag–Ag_2Se hybrid nanoparticles depend on the thickness of the Ag film in the Ag/Se thin-film structure, the concentration of Ag–Ag_2Se hybrid nanoparticles, and the annealing temperature. The synthesized hybrid Ag–Ag_2Se nanoparticles with high extinction coefficients and refraction indices may find use in various fields, such as the engineering of optical devices, sensors, and information storage devices.

Acknowledgments

The authors wish to thank T.N. Mogileva for technical assistance.

Equipment provided by the common use center of the Udmurt Federal Research Center (Ural Branch, Russian Academy of Sciences) was used in experiments.

Funding

This study was carried out under the state assignment of the Ministry of Science and Higher Education of the Russian Federation (state registration number 1021032422167-7-1.3.2).

Conflict of interest

The authors declare that they have no conflict of interest.

References

[1] V. Biju, T. Itoh, A. Anas, A. Sujith, M. Ishikawa, Anal. Bioanal. Chem., **391**, 2469 (2008). DOI: 10.1007/s00216-008-2185-7
[2] I. Boginskaya, A. Gainutdinova, A. Gusev, K. Mailyan, A. Mikhailitsyn, M. Sedova, A. Vdovichenko, A. Glushchenkov, A. Dorofeenko, I. Ryzhikov, Coatings, **11**, 1171 (2021). DOI: 10.3390/coatings11101171
[3] E. Prodan, P. Nordlander, J. Chem. Phys., **120** (11), 5444 (2004). DOI: 10.1063/1.1647518
[4] D.W. Brandl, N.A. Mirin, P. Nordlander, J. Phys. Chem. B, **110**, 12302 (2006). DOI: 10.1021/JP0613485
[5] J. Hranisavljevic, N.M. Dimitrijevic, G.A. Wurtz, G.P. Wiederrecht, J. Am. Chem. Soc., **124**, 4536 (2002). DOI: 10.1021/ja012263e
[6] V.S. Lebedev, A.D. Kondorskiy, Phys. Usp., **68**, 46 (2025). DOI: 10.3367/UFNe.2024.08.039742.
[7] V.S. Lebedev, A.G. Vitukhnovsky, A. Yoshida, N. Kometani, Y. Yonezawa, Coll. Surf. A, **326**, 204 (2008). DOI: 10.1016/j.colsurfa.2008.06.027
[8] M.R. Younis, C. Wang, R. An, S. Wang, M.A. Younis, Z.Q. Li, Y. Wang, A. Ihsan, D. Ye, X.H. Xia, ACS Nano, **13**, 2544 (2019). DOI: 10.1021/acsnano.8b09552
[9] K. Chen, L.L. Gong, S.J. Ding, J. Liu, S. Ma, J.H. Wang, D.J. Yang, G.M. Pan, Z.H. Hao, L. Zhou, Q.Q. Wang, Plasmonics, **15**, 21 (2020). DOI: 10.1007/s11468-019-01002-y
[10] H. Tang, Z.A. Chen, C. Ouyang, Z. Ye, S. Li, Z. Hong, M. Zhi, J. Phys. Chem. C, **126** (47), 20036 (2022). DOI: 10.1021/acs.jpcc.2c06373
[11] M. Ivanchenko, H. Jing, Chem. Mater., **35**, 4598 (2023). DOI: 10.1021/acs.chemmater.3c00346
[12] V.Ya. Kogai, G.M. Mikheev, JETP Lett., **120** (3), 190 (2024). DOI: 10.1134/S0021364024602458
[13] A.I. Sidorov, Tech. Phys., **51** (4), 477 (2006). DOI: 10.1134/S106378420604013X
[14] V.Ya. Kogai, Tech. Phys., **61** (3), 461 (2016). DOI: 10.1134/S1063784216030117
[15] V.Ya. Kogai, Tech. Phys. Lett., **44** (11), 1002 (2018). DOI: 10.1134/S1063785018110226
[16] J. Shin, J.T. Shen, S. Fan, Phys. Rev. Lett., **102**, 093903 (2009). DOI: 10.1103/PhysRevLett.102.093903

Translated by D.Safin